Formation of ultrashort triangular pulses in optical fibers

S. O. Iakushev,[1] O. V. Shulika,[2,*] I. A. Sukhoivanov,[2] V. I. Fesenko,[1,3] M. V. Andrés,[4] and H. Sayinc[5]

[1]*R&D Lab. "Photonics", Kharkiv National University of Radio Electronics, Ukraine*
[2]*Department of Electronic Engineering, DICIS, University of Guanajuato, Mexico*
[3]*Department of Microwave Electronics, Institute of Radio Astronomy of NASU, Ukraine*
[4]*Department of Applied Physics, University of Valencia, Spain*
[5]*Laser Development Department, Laser Zentrum Hannover, Hannover, Germany*

[*]*oshulika@ugto.mx*

Abstract: Specialty shape ultrashort optical pulses, and triangular pulses in particular, are of great interest in optical signal processing. Compact fiber-based techniques for producing the special pulse waveforms from Gaussian or secant pulses delivered by modern ultrafast lasers are in demand in telecommunications. Using the nonlinear Schrödinger equation in an extended form the transformation of ultrashort pulses in a fiber towards triangular shape is characterized by the misfit parameter under variety of incident pulse shapes, energies, and chirps. It is shown that short (1-2 m) conventional single mode fiber can be used for triangular pulse formation in the steady-state regime without any pre-chirping if femtosecond pulses are used for pumping. The pulses obtained are stable and demonstrate linear chirp. The ranges and combinations of the pulse parameters found here will serve as a guide for scheduling the experiments and implementation of various all-fiber schemes for optical signal processing.

OCIS codes: (190.4370) Nonlinear optics, fibers; (320.7110) Ultrafast nonlinear optics; (320.5540) Pulse shaping.

References and links

1. S. Boscolo and C. Finot, "Nonlinear pulse shaping in fibers for pulse generation and optical processing," Int. J. Optics **2012**, 1–14 (2012).
2. F. Parmigiani, P. Petropoulos, M. Ibsen, P. J. Almeida, T. T. Ng, and D. J. Richardson, "Time domain add-drop multiplexing scheme snhanced using a saw-tooth pulse shaper," Opt. Express **17**, 8362–8369 (2009).
3. F. Parmigiani, M. Ibsen, P. Petropoulos, and D. J. Richardson, "Efficient all-optical wavelength conversion scheme based on a saw-tooth pulse shaper," IEEE Photon. Technol. Lett. **21**, 1837–1839 (2009).
4. A. I. Latkin, S. Boscolo, R. S. Bhamber, and S. K. Turitsyn, "Doubling of optical signals using triangular pulses," J. Opt. Soc. Am. B **26**, 1492–1496 (2009).
5. R. S. Bhamber, S. Boscolo, A. I. Latkin, and S. K. Turitsyn, "All-optical TDM to WDM signal conversion and partial regeneration using XPM with triangular pulses," in "Optical Communication, 2008. ECOC 2008. 34th European Conference on," (Brussels, Begium, 2008).
6. A. M. Weiner, "Femtosecond pulse shaping using spatial light modulators," Rev. Scien. Instrum. **71**, 1939–1960 (2000).
7. A. M. Clarke, D. G. Williams, M. A. F. Roelens, and B. J. Eggleton, "Reconfigurable optical pulse generator employing a Fourier-domain programmable optical processor," J. Lightwave Technol. **28**, 97–103 (2010).
8. D. Nguyen, M. U. Piracha, D. Mandridis, and P. J. Delfyett, "Dynamic parabolic pulse generation using temporal shaping of wavelength to time mapped pulses," Opt. Express **19**, 12305–12311 (2011).
9. J. Ye, L. Yan, W. Pan, B. Luo, X. Zou, A. Yi, and S. Yao, "Photonic generation of triangular-shaped pulses based on frequency-to-time conversion," Opt. Lett. **36**, 1458–1460 (2011).

#224299 - $15.00 USD Received 2 Oct 2014; revised 1 Nov 2014; accepted 1 Nov 2014; published 14 Nov 2014

10. P. Petropoulos, M. Ibsen, A. D. Ellis, and D. J. Richardson, "Rectangular pulse generations based on pulse reshaping using a superstructured fiber bragg grating," J. Lightwave Technol. **19**, 746–752 (2001).
11. T. Hirooka, M. Nakazawa, and K. Okamoto, "Bright and dark 40 GHz parabolic pulse generation using a picosecond optical pulse train and an arrayed waveguide grating," Opt. Lett. **33**, 1102–1104 (2008).
12. C. Finot, L. Provost, P. Petropoulos, and D. J. Richardson, "Parabolic pulse generation through passive nonlinear pulse reshaping in a normally dispersive two segment fiber device," Opt. Express **15**, 852–864 (2007).
13. S. Boscolo, A. I. Latkin, and S. K. Turitsyn, "Passive nonlinear pulse shaping in normally dispersive fiber systems," IEEE J. Quantum Electron. **44**, 1196–1203 (2008).
14. S. O. Iakushev, O. V. Shulika, and I. A. Sukhoivanov, "Passive nonlinear reshaping towards parabolic pulses in the steady-state regime in optical fibers," Opt. Commun. **285**, 4493–4499 (2012).
15. I. A. Sukhoivanov, S. O. Iakushev, O. V. Shulika, A. Díez, and M. Andrés, "Femtosecond parabolic pulse shaping in normally dispersive optical fibers," Opt. Express **21**, 17769–17785 (2013).
16. H. Wang, A. I. Latkin, S. Boscolo, P. Harper, and S. K. Turitsyn, "Generation of triangular-shaped optical pulses in normally dispersive fibre," J. Opt. **12**, 035205–1–5 (2010).
17. N. Verscheure and C. Finot, "Pulse doubling and wavelength conversion through triangular nonlinear pulse reshaping," Electron. Lett. **47**, 1194–1196 (2011).
18. G. P. Agrawal, *Nonlinear Fiber Optics* (Academic, 2007), 4th ed.
19. A. Zeytunyan, G. Yesayan, L. Mouradian, P. Kockaert, P. Emplit, F. Louradour, and A. Barthélémy, "Nonlinear-dispersive similariton of passive fiber," J. Euro. Opt. Soc. - Rapid Pub. **4**, 09009–1–7 (2009).
20. A. Tomlinson, R. H. Stolen, and C. V. Shank, "Compression of optical pulses chirped by self-phase modulation in fibers," J. Opt. Soc. Am. B **1**, 139–149 (1984).
21. M. Karlsson, "Optical fiber-grating compressors utilizing long fibers," Opt. Commun. **112**, 48–54 (1994).
22. S. Boscolo and S. K. Turitsyn, "Intermediate asymptotics in nonlinear optical systems," Phys. Rev. A **85**, 043811 (2012).
23. S. Ramachandran, *Fiber Based Dispersion Compensation* (Springer, 2007).
24. Thorlabs, "Specification sheet: 780 HP – Single Mode Optical Fiber, 780 – 970 nm, ⌀ 125 μm cladding (Rev. D, 2013-April-1, 6829-s01)," http://www.thorlabs.com/thorcat/6800/780HP-SpecSheet.pdf (2013). Accessed: 2014-June-27.
25. OFS, "TrueWave Ocean Fibers SRS," http://ofsoptics. thomasnet-navigator.com/Asset/TrueWaveSRSFiber-121-web.pdf (2013). Accessed: 2014-June-27.
26. B. B. Bale, S. Boscolo, K. Hammani, and C. Finot, "Effects of fourth-order fiber dispersion on ultrashort parabolic optical pulses in the normal dispersion regime," J. Opt. Soc. Am. B **28**, 2059–2065 (2011).

1. Introduction

Ultrashort optical pulses of special waveforms are very important in a number of scientific applications, including ones in all-optical signal processing and manipulation, ultra-high-speed optical systems, nonlinear and quantum optics [1]. The state of the art ultrafast lasers deliver usually Gaussian or secant pulse waveforms. However, many practical applications require employment of larger variety of pulse waveforms such as flat-top (rectangular-like), parabolic, and triangular pulses. Particularly, triangular pulses have found numerous applications in time domain add-drop multiplexing [2], wavelength conversion [3], optical signal doubling [4], time-to-frequency mapping of multiplexed signals [5]. Therefore the development of simple and efficient optical approaches for picosecond and sub-picosecond pulse reshaping is an actual task. Conventional optical pulse shaping in picosecond and femtosecond time scales implies direct filtering of pulse amplitude and phase in spectral domain or in temporal one [6–11]. This technique requires application of special devices such as acousto-optic spatial light modulators or those one based on liquid crystals, fiber Bragg gratings, arrayed waveguide gratings [6–11].

In order to fulfill requirements of telecommunications, the compact fiber-based techniques for producing the special pulse waveforms from Gaussian or secant pulses delivered by modern ultrafast lasers are required. Another approach based on the nonlinear pulse reshaping in normally dispersive optical fibers has been also proposed. And it was shown that this approach allows obtaining ultrashort parabolic waveform [12–15] via combined action of self-phase modulation (SPM) and normal dispersion (ND) on the pulse shape and spectrum during pulse propagation in single mode normal dispersion fibers. As it was demonstrated this approach could also provide triangular pulse formation [13, 16]. Particularly it was shown that triangular pulses can

#224299 - $15.00 USD Received 2 Oct 2014; revised 1 Nov 2014; accepted 1 Nov 2014; published 14 Nov 2014

be obtained from Gaussian pulses having specific chirp and energy, within the narrow range of the fiber lengths up to one dispersion length. Also the picosecond triangular pulse formation was experimentally demonstrated applying long 2-4 km normal dispersion fiber for pulse reshaping and 400-700 m fiber with anomalous dispersion for pre-chirping [16]. The same scheme has been applied in [17] with secant hyperbolic incident pulses.

However, the conditions of triangular pulse formation in normal dispersive fibers are still not fully understood. Here we investigate via numerical modeling formation of triangular pulses in normally dispersive fibers under variety of conditions: different initial pulse shapes, large variation of the fiber length, initial chirp and soliton order. Special attention is focused on the formation of stable triangular pulses which can preserve the triangular shape and triangular spectrum during propagation in the fiber over the long distance. We expand here our approach proposed previously for formation of stable parabolic pulses via passive nonlinear reshaping in normal dispersion optical fibers [14, 15] to the triangular waveforms formation. We show that this approach allow implementation of the compact fiber-based schemes (1-2 m of conventional normal dispersion fiber) of triangular pulse formation in the steady-state propagation regime without any pre-chirping stage from Gaussian or secant femtosecond pulses delivered by conventional ultrafast lasers. This approach is much simpler for implementation and device development.

2. Theoretical description of pulse transformation under propagation in a fiber

The formation of the nearly triangular pulses in the normal dispersion optical fibers is governed by the interplay of normal group velocity dispersion and nonlinearity. This fundamental mechanism is the same as for passive nonlinear reshaping to parabolic pulses [12–15] and well described by the nonlinear Schrödinger equation (NLSE) [18]. However, here we extend standard NLSE by including the fiber loss and the third-order dispersion in order to take into account parameters of real fibers. Thus, the nonlinear Schrödinger equation (NLSE) of the following form is used to describe the evolution of an ultrashort pulse during its propagation in a normal-dispersion optical fiber with Kerr nonlinearity:

$$\frac{\partial A}{\partial z} = -\frac{\alpha}{2}A - i\frac{\beta_2}{2}\frac{\partial^2 A}{\partial T^2} + \frac{\beta_3}{6}\frac{\partial^3 A}{\partial T^3} + i\gamma|A|^2 A, \tag{1}$$

where A is the slowly varying complex envelope of the pulse; α is the losses; β_2 is the second order dispersion; β_3 is the third order dispersion; γ is the nonlinear coefficient; T is the time in a co-propagating time-frame; z is the propagation distance. In Eq. (1), the dispersion coefficients β_n are accounted for by expanding the mode-propagation constant $\beta(\omega)$ in a Taylor series around the frequency ω_0 at which the pulse spectrum is centered:

$$\beta(\omega) = \widetilde{n}_{eff}\frac{\omega}{c} = \sum_{n\geqslant 0}\frac{1}{n!}\frac{\partial^n \beta(\omega_0)}{\partial \omega^n}(\omega-\omega_0) \tag{2}$$

The Eq. (1) is solved numerically using the split-step Fourier method [18]. For the subsequent discussion it is convenient to use following notations for the dispersion length L_D , nonlinear length L_{NL}, soliton order N, and normalized distance ξ:

$$L_D = \frac{T_0^2}{|\beta_2|}, \quad L_{NL} = \frac{1}{\gamma P_0}, \quad N = \sqrt{\frac{L_D}{L_{NL}}}, \quad \xi = \frac{z}{L_D}. \tag{3}$$

In these expressions, P_0 is the initial pulse peak power, T_0 is the initial pulse duration (half-width at $1/e$ intensity level).

#224299 - $15.00 USD Received 2 Oct 2014; revised 1 Nov 2014; accepted 1 Nov 2014; published 14 Nov 2014

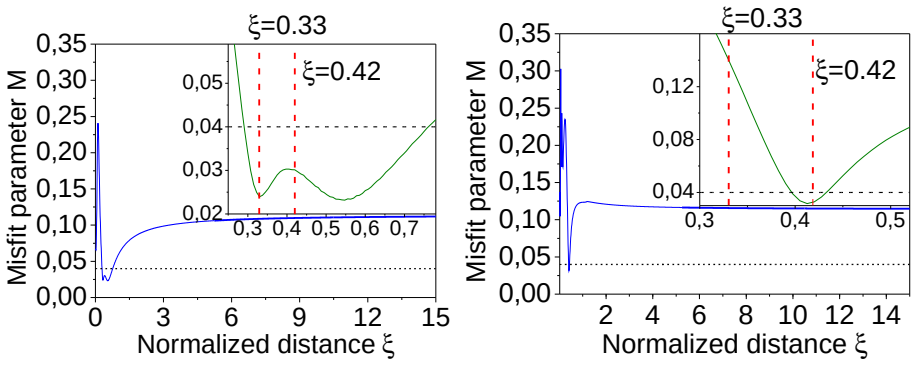

(a) (b)

Fig. 1. Evolution of the misfit parameter M versus normalized distance ξ for the temporal (a) and spectral (b) pulse shapes at $N = 10$ and $C = -4$, which corresponds to the case example of [16] shown there on Fig. 1. Black dashed lines correspond to the level $M = 0.04$. The insets in the figures show the enlarged areas of the minima where $M < 0.04$.

The quality of the triangular pulse is estimated through the deviation of its temporal intensity profile $|A(T)|^2$ and a triangular fit $|A_\Delta(T)|^2$ of the same energy; it characterizes quantitatively via the misfit parameter M [16]:

$$M = \frac{\int \left(|A|^2 - |A_\Delta|^2\right)^2 \partial T}{\int |A|^4 \partial T}. \tag{4}$$

We use the following expression for the triangular fit of the pulse envelope $A_\Delta(T)$ of the energy $E_\Delta = P_\Delta T_\Delta \sqrt{2.5}$

$$A_\Delta(T) = \begin{cases} \sqrt{P_\Delta}\sqrt{1 - \left|\frac{T}{T_\Delta\sqrt{2.5}}\right|}, & |T| \leqslant T_\Delta\sqrt{2.5} \\ 0, & otherwise \end{cases} \tag{5}$$

where P_Δ is the peak power of the triangular pulse, T_Δ is the duration of the triangular pulse (the half-width at 1/e intensity point). The misfit parameter M allows estimating the pulse shape imperfection quntitavtively as compared to the triangular shape; a smaller value of M shows better fit to the triangular waveform. Usually we can consider a pulse shape to be close enough to the triangular one when $M < 4\%$.

Results presented in this paper are obtained for both an unchirped and chirped pulses. We include the chirp into the initial pulse in the following way:

$$A_{chirp} = A_0 \exp\left(iC\frac{T^2}{2T_0^2}\right), \tag{6}$$

where A_0 and A_{chirp} are the waveform of an unchirped and chirped initial pulse, respectively; C is the chirp parameter. Adding the chirp in this way leads to the linear dependence of instantaneous frequency defined as:

$$\omega = \omega_0 + C\frac{T}{T_0^2}. \tag{7}$$

#224299 - $15.00 USD Received 2 Oct 2014; revised 1 Nov 2014; accepted 1 Nov 2014; published 14 Nov 2014

The instantaneous frequency in this case increases linearly from the leading to the trailing edge of the pulse for $C > 0$ (positive chirp) while the opposite process occurs for $C < 0$ (negative chirp).

3. Triangular pulse formation in the transient-state and steady-state propagation regimes

The passive nonlinear pulse reshaping in normally dispersive fibers is governed by the interplay between SPM and group velocity dispersion (GVD). Here one can mark out two propagation regimes previously studied for parabolic pulse formation [12–15]. The first one implies formation of the pulses of particular shape at the short propagation distance in the fiber usually shorter than the dispersion length ($\xi < 1$) [12, 13]. In this case pulse reshaping appears under strong action of SPM, which at first leads to fast changes of the pulse shape and its spectrum, and usually results in rather nonlinear pulse chirp. The desired pulse shape can be achieved here within the narrow range of the fiber lengths; however, further pulse propagation in the fiber leads, in general case, to the change of the pulse shape. Therefore, we term this regime of pulse formation as a transient-state propagation (TSP) regime throughout the paper. Formation

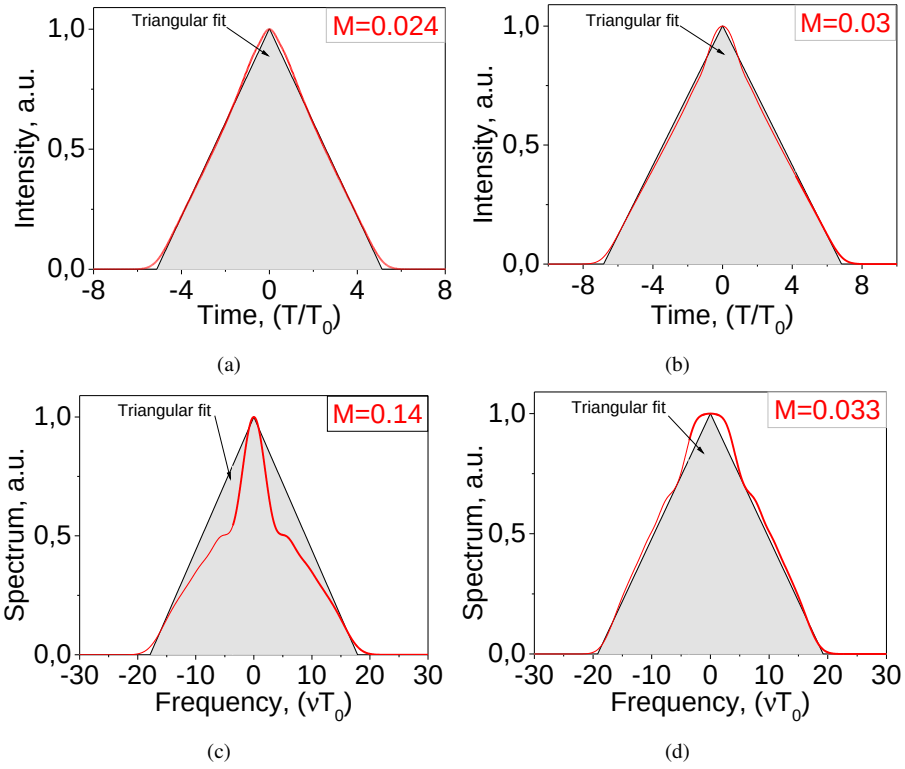

Fig. 2. Normalized pulse temporal intensity (a), (b) and spectrum (c), (d) in the transient-state propagation (TSP) regime produced from chirped Gaussian pulse ($N = 10$, $C = -4$) at the distances $\xi = 0.33$ (the left column) and $\xi = 0.42$ (the right column), respectively. The right column corresponds to the case example of [16] shown there on Fig. 1. The insets located in the upper right corner show the value of misfit parameter M. Red curves show corresponding triangular fits.

#224299 - $15.00 USD Received 2 Oct 2014; revised 1 Nov 2014; accepted 1 Nov 2014; published 14 Nov 2014

of triangular pulses reported in [16] is achieved exactly in the TSP-regime.

Another mode of pulse formation in normally dispersive fiber is the steady-state propagation (SSP) regime [14, 15]. It implies formation of pulses of a particular shape at a longer propagation distance which usually exceeds a few dispersion lengths, and can be expressed roughly by $\xi > 1$. The pulse reshaping in this case occurs under much weaker action of SPM and domination of GVD. In this regime pulse gains spectronic properties [19]. Particularly the pulse shape repeats its spectrum profile and the chirp of the pulse becomes perfectly linear. In this regime the spectral width of the pulse approaches its maximum asymptotic value leading to the saturation of the pulse compression factor [20] and achievement of maximal compression [21]. We term this regime as the steady-state one, because of both the pulse temporal profile and the spectral profile are changing very slowly and are actually approaching some limit. Triangular shape pulses, like those one formed passive fibers in SSP-regime, can also be generated in active systems like mode-locked fiber lasers, as has been discussed in [22].

As we just pointed out, duration of SSP-produced pulses will be larger as compared to TSP-produced ones, due to the large temporal broadening undergone in the first case; it could be an issue for high repetition rate signal. However, this possible issue can be overcame within the all-fiber (or in-fiber) implementation using variety of accessible concepts [23].

The ultimate goal of this paper is to find detailed conditions of the triangular pulse formation both in the transient-state propagation regime and in the steady-state propagation regime.

We start from the combination of parameters for triangular pulse formation in the TSP-regime presented in [16]. It will serve as a benchmark for our simulations and also will allow us highlighting the problem in hands. The M-plots shown in Fig. 1 demonstrate the dependence of the misfit parameter M versus the normalized length ξ for both the temporal Fig. 1(a) and spectral Fig. 1(b) pulse shapes for fixed values of the soliton order $N = 10$ and chirp parameter $C = -4$. Note, that another definitions of the normalized chirp parameter was used in [16] (scaling factor is -2). In case of spectral profile the Eqs. (4) and (5) are applied to the spectral pulse amplitude instead of temporal waveforms. Pulse shape and spectrum for these parameters at the fiber length $\xi = 0.33$ as well as triangular fits are shown in Fig. 2(a) and Fig. 2(c). These results are in good agreement with [16]. We can see that at $\xi = 0.33$ the pulse shape indeed is very close to the ideal triangular waveform ($M = 0.024$), but spectral profile here considerably differs from triangular one ($M = 0.14$). However, from Fig. 1 we can see that at fiber length $\xi = 0.42$ there is a minimum for spectral profile deviation where $M < 0.04$. From Fig. 2(b) and Fig. 2(d) we can see that indeed pulse shape and spectrum are both close to the ideal triangular profile at the distance $\xi = 0.42$.

Thus, in the TSP-regime one can find the region of the fiber lengths where both temporal and spectral profiles are close to the triangular shape. However, these regions of the fiber lengths (where $M < 0.04$) are very narrow. For the temporal profile we have $0.29 < \xi < 0.76$, whereas for spectral profile it is $0.396 < \xi < 0.432$. Further pulse propagation in the fiber leads to strong and rapid deviation from the triangular profile as Fig. 1 clearly shows. Thus, in the SSP-regime we cannot obtain a triangular pulse for given parameters. Therefore, detailed analysis of the conditions of triangular pulse formation both in TSP- and in SSP-regimes is required.

4. The impact of the soliton order

Soliton order (or soliton number, energy parameter) N appears originally in the soliton theory in the anomalous dispersion region of the fibers. However, in the normal dispersion region it is still useful, because it shows the relative strength of SPM and GVD action on the pulse in the fiber [18]. We consider in this paper the case when $N > 1$, such that the impact of SPM is larger as compared to GVD over at least a few stages of pulse evolution in the fiber. This provides nonlinear reshaping of the pulse shape in the fiber. Larger number on N provides stronger

#224299 - $15.00 USD Received 2 Oct 2014; revised 1 Nov 2014; accepted 1 Nov 2014; published 14 Nov 2014

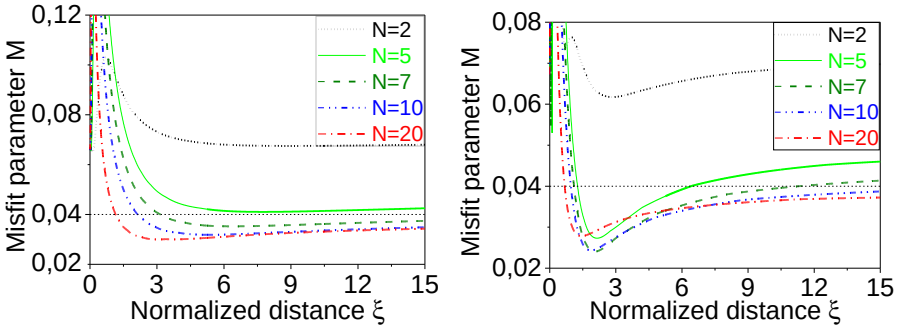

Fig. 3. Evolution of the misfit parameter M versus normalized distance ξ for the temporal (a) and spectral (b) pulse shapes in case of the initial *unchirped* Gaussian pulse.

impact of SPM. Whereas in the case $N \leqslant 1$ dispersion dominates (linear case) and nonlinear pulse reshaping is not sufficient. We calculated the M-plots, which represent the dependence of the misfit parameter M on the normalized distance ξ for various values of the soliton order N . Results presented here were obtained for the case of initially unchirped ($C = 0$) pulses with different initial shapes: the Gaussian, the hyperbolic-secant, and the super-Gaussian. The Gaussian and the secant pulses are typically emitted by modern ultrafast lasers, whereas the super-Gaussian waveform allows usually modeling of pulses with steeper edges as compared to the conventional Gaussian pulse.

Let us first consider the pulse reshaping in case of the initial Gaussian pulse shape, shown in Fig. 3. We show here only dependencies of $M(\xi)$ for temporal waveforms, because the triangular temporal shape is more important from the practical point of view. One has to note that in the steady-state regime temporal and spectral shapes always repeat each other, whereas in the transient-state regime they coincide rarely. From Fig. 3 we can see that there is not any minimum in the range $\xi < 1$, i.e. we cannot achieve triangular waveform for these conditions in TSP-regime. Whereas in SSP-regime ($\xi > 1$) the pulse shape can be quite diverse, depending on the N . Notably, the misfit parameter M decreases considerably with increasing of the soliton order N that leads to decreasing of deviation from the triangular shape. Fig. 3 shows that misfit

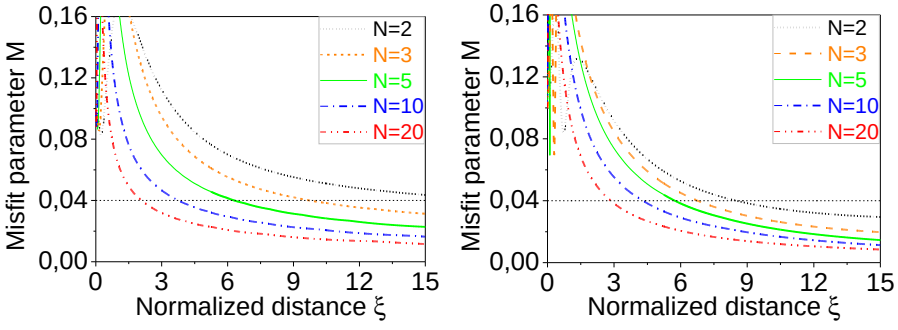

Fig. 4. Evolution of the misfit parameter M versus normalized distance ξ for the temporal (a) and spectral (b) pulse shapes in case of the initial *unchirped* secant hyperbolic pulse.

#224299 - $15.00 USD Received 2 Oct 2014; revised 1 Nov 2014; accepted 1 Nov 2014; published 14 Nov 2014

parameter achieves a magnitude less than 4% at $N \geqslant 7$. Besides, as follows from these plots, the required distance to achieve a fully triangular pulse shape ($M < 0.04$) is decreasing with increasing of N. For example, these distances are $\xi = 2.14$ at $N = 10$ and $\xi = 1.14$ at $N = 20$. Next, we consider pulse reshaping in case of initial hyperbolic secant pulse shape, which is shown in Fig. 4. In transient-state propagation regime we also cannot achieve triangular waveform. However, in steady-state propagation regime pulse reshaping process provides formation of triangular pulse ($M < 0.04$) for smaller values of soliton order as compared to the initial Gaussian pulse, starting already from $N \geqslant 3$. Moreover, the value of misfit parameter M in the steady-state regime is smaller as compared to the initial Gaussian pulse. Thus, application of secant pulses is preferable for obtaining triangular pulses in the steady-state. However, one has to note that the minimal distance required for triangular pulses to be formed in the steady-state regime is slightly larger for a given value of soliton order as compared to the initial Gaussian pulse. For example, these distances are $\xi = 3.75$ at $N = 10$ and $\xi = 2.07$ at $N = 20$.

Now we address pulse reshaping when the initial pulse possesses third-order super-Gaussian shape. The corresponding M-plots are shown in Fig. 5. We can see that in the steady-state regime we cannot achieve triangular waveform from super-Gaussian pulse by changing the soliton order. However, in the transient-state regime (see Fig. 5(c)) one can see the appearance of minima ($M \leqslant 0.04$) for $7 \leqslant N \leqslant 15$. Thus, in this case we can obtain triangular pulses in

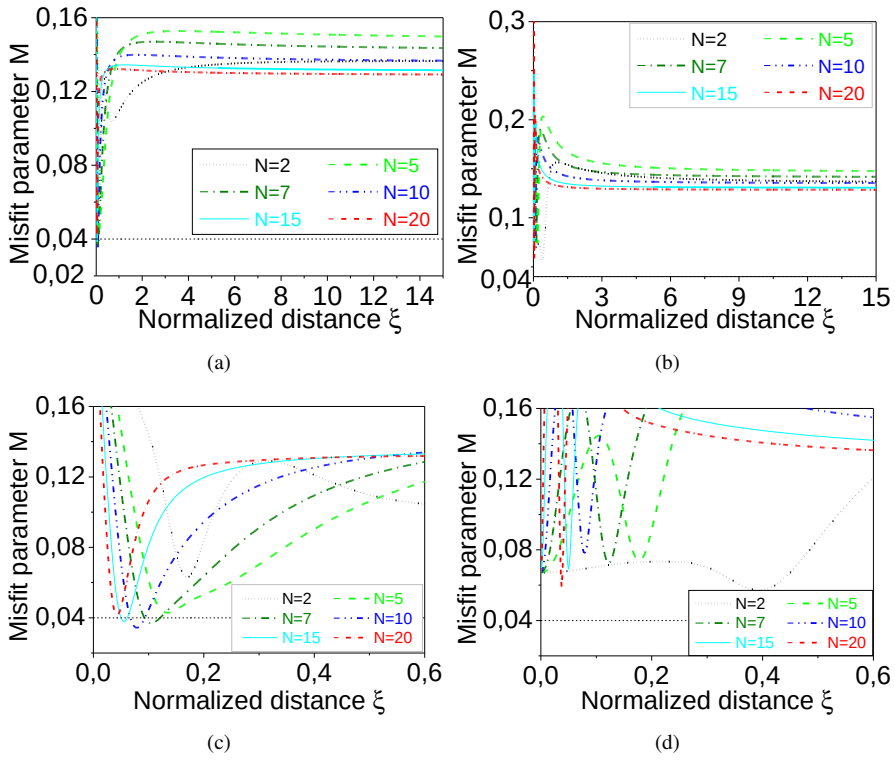

Fig. 5. Evolution of the misfit parameter M versus ξ for temporal (a) and spectral (b) pulse shapes in case of the initial *unchirped* 3-rd order super-Gaussian pulse. Figures (c) and (d) shows the enlarged areas of the minima of M in the transient-state propagation (TSP) regime extracted from Fig. 5(a) and Fig. 5(b), respectively.

#224299 - $15.00 USD Received 2 Oct 2014; revised 1 Nov 2014; accepted 1 Nov 2014; published 14 Nov 2014

temporal domain, but corresponding spectral profiles are noticeably diverging from triangular waveform (see Fig. 5(d)).

Thus, the soliton order has significant influence on the pulse reshaping process, and, thus, can be used to control this transformation. In the transient-state regime variation of the soliton order in the case of unchirped pulses provides formation of triangular pulses only from initial super-Gaussian (3-rd order) pulse when $7 \leqslant N \leqslant 15$. Whereas initial unchirped Gaussian or secant pulses do not transform to the triangular waveform in the transient-state regime. The opposite appears in the steady-state regime. Here the variation of soliton order allows producing of triangular pulses from initial unchirped Gaussian pulse ($N \geqslant 7$) and from secant pulse ($N \geqslant 3$). Whereas initial unchirped super-Gaussian (3-rd order) pulse does not transform to the triangular waveform in the steady-state regime.

5. The impact of the initial pulse chirp

Results presented above, in Sec. 4, were obtained under in-coupling of unchirped pulses, *i.e.* when $C = 0$; now we examine an influence of both positive ($C > 0$) and negative ($C < 0$) initial pulse chirps on the pulse reshaping towards triangular waveform. As before, we consider various initial pulse shapes (Gaussian, secant hyperbolic, and super-Gaussian) and a wide range of initial chirp values up to $|C| = 12$. Larger values of the chirp parameter C are related already to significant dispersion broadening. The soliton order was chosen to be $N = 10$ in this section, in order to meet all the conditions of Sec. 4.

At first the pulse evolution for the initial Gaussian pulse is considered. The M-plots presented in Fig. 6 demonstrate the dependence of the misfit parameter M on the normalized distance ξ for various values of chirp parameter C for the temporal Figs. (6(a), 6(c), 6(e)) and spectral Figs. (6(b), 6(d), 6(f)) pulse profiles. From these figures we can see that the initial chirp is able to change significantly pulse evolution as compared to the unchirped initial pulse ($C = 0$). At first, in the transient-state propagation regime one can see the appearance of minima ($M \leqslant 0.04$) for negative values of chirp. Fig. 6(c) clearly shows that triangular pulses can be achieved in the transient-state regime ($\xi < 1$) when $-8 \leqslant C \leqslant -2$. The best choice is $C = -2$ at $\xi = 1$: here the misfit parameter is the smallest one ($M = 0.015$) and spectral profile is also close to the ideal triangular waveform. Increasing the amount of negative chirp leads to the shifting of the minima to the smaller values of ξ and larger values of M. One has to note that for $N = 3$ even adding initial negative chirp dos not lead to the triangular pulse formation as Fig. 6(e) shows. Therefore, the necessary condition for triangular pulse formation from Gaussian pulses with negative chirp in the transient-state propagation regime is $N > 3$.

In the steady-state propagation regime (see Fig. 6(a) and Fig. 6(c)) we can see that, in general, the adding of the initial positive or negative chirp increases the deviation form triangular waveform as compared to unchirped initial pulse. However, there is the range of initial chirp $-0.5 \leqslant C \leqslant 0.4$ where the pulse in the steady-state propagation regime preserves triangular profile both in temporal and spectral domains. Adding a small negative chirp ($C \sim -0.5$) is even preferable allowing to slightly reduce the distance of triangular pulse formation in the steady-state regime ($\xi \sim 1.5$).

Now we consider the impact of initial chirp on reshaping of secant hyperbolic pulse towards triangular waveform, shown in Fig. 7. Here one can see that the adding of initial chirp does not lead to the formation of triangular pulses in the transient-state regime. In the steady-state regime the adding of the initial chirp also increases the deviation form triangular waveform as compared to unchirped initial pulse similarly to the Fig. 6. Within the following range of initial chirp $-0.8 \leqslant C \leqslant 0.5$ pulse preserves triangular profile both in temporal and spectral domain in the stead-state regime.

Finally we investigate the impact of initial chirp on the triangular pulse formation from the

#224299 - $15.00 USD Received 2 Oct 2014; revised 1 Nov 2014; accepted 1 Nov 2014; published 14 Nov 2014

initial super-Gaussian (3-rd order) pulse. From Fig. 8 one can see that in the steady-state regime the adding of initial chirp cannot provide formation of triangular pulse. In the transient-state regime the triangular pulse which is formed from unchirped super-Gaussian pulse remains perfectly stable against adding of initial chirp (see Fig. 8(c)). Namely, the triangular waveform can

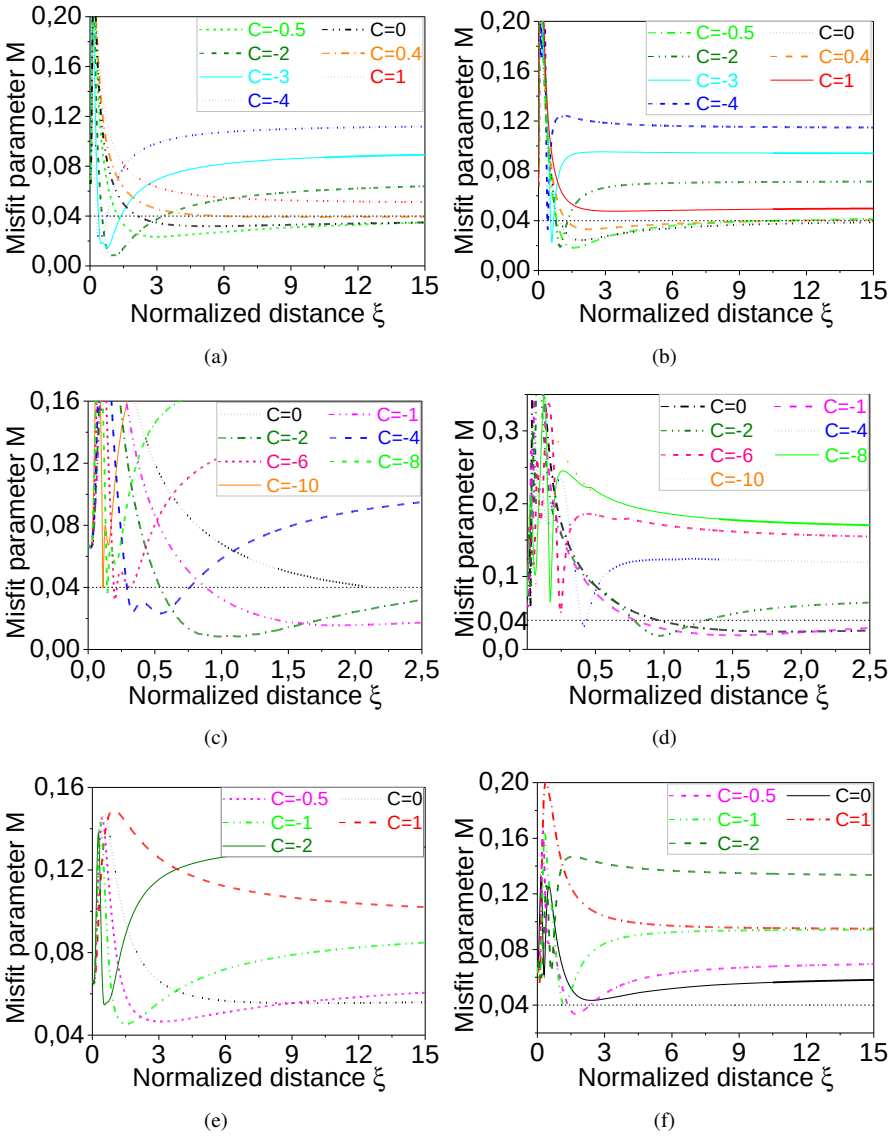

Fig. 6. Evolution of the misfit parameter M versus ξ for temporal (a) and spectral (b) pulse shapes in case of the initial Gaussian pulse having $N = 10$. Figures (c) and (d) show the enlarged areas of the minima of M in the transient-state propagation (TSP) regime extracted from Fig. 6(a) and Fig. 6(b), respectively. Fig. 6(e) and Fig. 6(f) shows evolution of the misfit parameter M versus ξ for temporal and spectral pulse shapes, respectively, in case of the initial Gaussian pulse with $N = 3$.

#224299 - $15.00 USD Received 2 Oct 2014; revised 1 Nov 2014; accepted 1 Nov 2014; published 14 Nov 2014

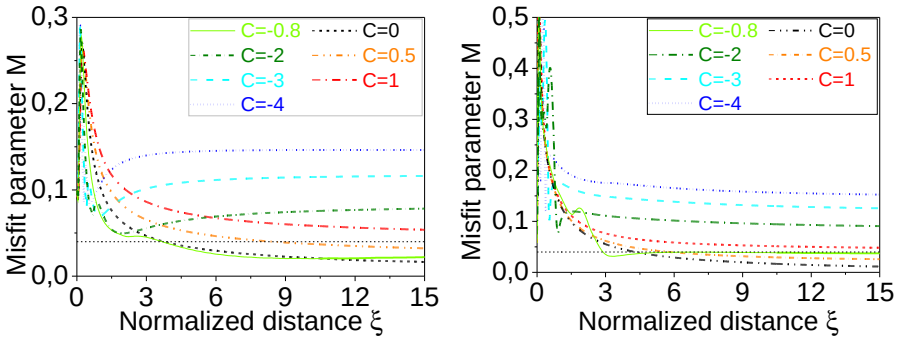

Fig. 7. Evolution of the misfit parameter M versus normalized distance ξ for the temporal (a) and spectral (b) pulse shapes in case of the initial secant hyperbolic pulse with $N = 10$ and various values of chirp.

be achieved for a large range of negative chirp (at least up to $C = -12$) , in case of positive chirp triangular waveform can be achieved for the maximal amount $C = 4$.

We can conclude that the impact of initial chirp on the pulse reshaping is also significant. In the transient-state regime the addition of an initial chirp allows the generation of triangular pulses from initial Gaussian pulses, particularly for $N = 10$ one has to apply chirp in the following range $-8 \leqslant C \leqslant -2$. However, the necessary condition in this case is $N > 3$, a smaller value of the soliton order does not provide triangular pulse formation even after the adding of negative initial chirp. Secant initial pulses do not transform to the triangular waveform in the transient-state propagation regime at all regardless of the initial chirp. As regards the super-Gaussian pulse, the triangular waveform is achieved here already from unchirped pulse. Triangular pulse formation in this case is preserved after the adding of initial chirp in the wide range, for $N = 10$ it is $-12 \leqslant C \leqslant 4$.

In the steady-state propagation regime in general, the adding of initial chirp increases the deviation form triangular waveform as compared to unchirped initial pulses. However, there is also the range of initial chirp $-0.5 \leqslant C \leqslant 0.4$ for initial Gaussian pulse and $-8 \leqslant C \leqslant 0.5$ for initial secant pulse where pulse in the stead-state regime preserves triangular profile both in temporal and spectral domains. Whereas for super-Gaussian pulse the adding of initial chirp does not lead to the triangular pulse formation in the stead-state propagation regime.

6. Practical recommendations for triangular pulse formation in optical fibers

Finally we are discussing some practical conditions required for triangular pulse formation in optical fibers. From the presented above results one can see that triangular pulses in the transient-state propagation regime can be obtained only from Gaussian or super-Gaussian pulses (3-rd order). As modern ultrafast lasers generate mostly Gaussian or secant pulses, the application of initial Gaussian pulse in this case is the most preferable. The necessary condition for triangular pulse formation is large enough amount of pulse energy, *i.e.* the soliton order N shall be sufficiently large: It is $N > 3$ in transient-state propagation regime for the incident pulse of the Gaussian shape. Another necessary condition is negative chirp of a particular value: for example for $N = 10$ one needs $-8 \leqslant C \leqslant -2$. Therefore, one has to provide a pre-chirping stage by using anomalous dispersion fiber [16] or other dispersion elements before the nonlinear reshaping of the pulse in normally dispersive fiber.

In steady-state propagation regime triangular pulses can be obtained from both the Gaussian

#224299 - $15.00 USD Received 2 Oct 2014; revised 1 Nov 2014; accepted 1 Nov 2014; published 14 Nov 2014

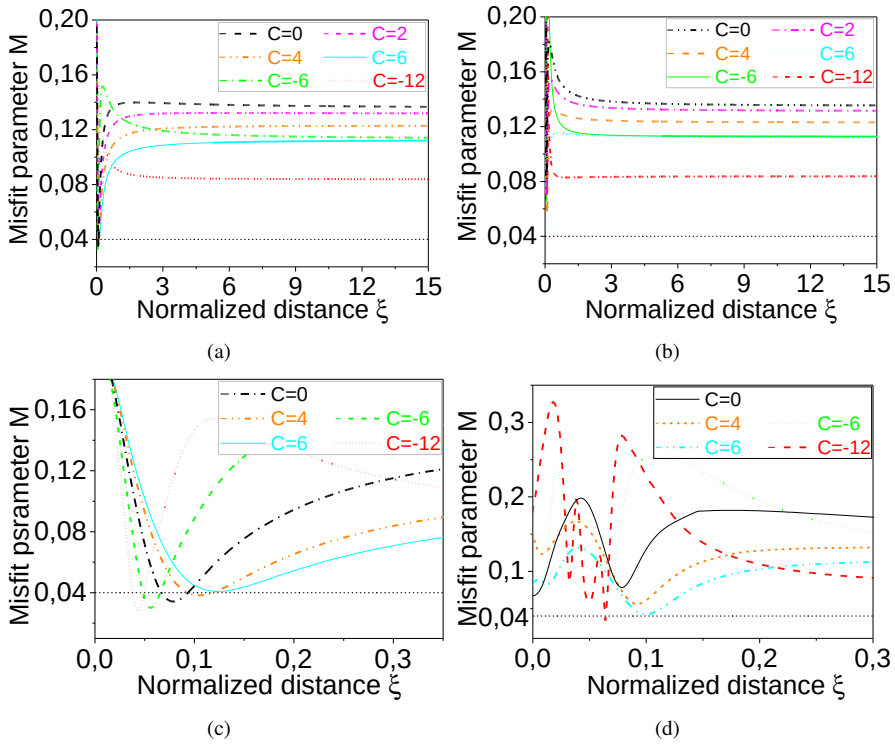

Fig. 8. Evolution of the misfit parameter M versus normalized distance ξ for the temporal (a) and spectral (b) pulse shapes in case of the initial super-Gaussian pulse with $N = 10$ and various values of chirp C. Fig. 8(c) and Fig. 8(d) show the enlarged areas of the minima in the transient-state propagation regime extracted from figures Fig. 8(a) Fig. 8(b), respectively.

and the secant hyperbolic initial pulses. The necessary conditions for triangular pulse formation in the steady-state propagation regime are: $N \geqslant 7$ for Gaussian pulse and $N \geqslant 3$ for secant hyperbolic pulse. Because of unchirped pulses can be used for triangular pulse formation in the steady-state regime, there is no need to provide a pre-chirping stage here. Initial chirp in this case is rather negative factor because it increases the deviation form the triangular waveform as compared to unchirped initial pulses. However, there is the range of initial chirp where pulse shape remains triangular in the steady-state propagation regime. For $N = 10$ these regions are $-0.5 \leqslant C \leqslant 0.4$ for initial Gaussian pulse, and $-0.8 \leqslant C \leqslant 0.5$ for initial secant hyperbolic pulse. We have combined the conditions for triangular pulse formation all together in Table 1.

Important issue is the duration of the initial pulses. If picosecond Gaussian pulses (e.g. ~ 5 ps) are used in a typical single mode fiber, such as Thorlabs 780HP [24], then, for example, at $\lambda = 1064$ nm ($\beta_2 = 25$ ps^2/km) the dispersion length is $L_D = 360$ m. It means that required fiber length for triangular pulse formation in the transient-state regime ($0.1L_D < z < L_D$) is in the range $36 < z < 360$ m, whereas in the steady-state propagation regime ($z > L_D$) the required fiber length has to be larger of 360 m. At $\lambda = 1550$ nm the normal dispersion in a single mode fiber is smaller. For example, the TrueWave fiber [25] has $\beta_2 = 4$ ps^2/km, and this provides dispersion length $L_D = 2.2$ km. Thus, one can see that application of picosecond initial pulses requires long fibers for pulse reshaping from a few hundred meters up to a few kilometers. If pi-

#224299 - $15.00 USD Received 2 Oct 2014; revised 1 Nov 2014; accepted 1 Nov 2014; published 14 Nov 2014

Table 1. Summary of the conditions for the formation of triangular pulses in a fiber.

Incident pulse shape	Transient-state propagation (TSP) regime	Steady-state propagation (SSP) regime
Gaussian	$N > 3$, with negative initial chirp in quite wide range corresponding to particular value of N.	$N \geqslant 7$, unchirped or slightly chirped in the narrow range corresponding to particular value of N.
	E. g. $N = 10$, $-8 \leqslant C \leqslant -2$. Example for particular value $C = -4$ shown in Fig. 2	*E. g.* $N = 10$, $-0.5 \leqslant C \leqslant 0.4$. Example for particular values $N = 7$, $C = 0$ shown in Fig. 9(a), 9(c))
Secant hyperbolic	–	$N \geqslant 3$, unchirped or slightly chirped in the narrow range corresponding to particular value of N.
		E. g. $N = 10$, $-0.8 \leqslant C \leqslant 0.5$. Example for particular values $N = 6$, $C = 0$ shown in Fig. 9(b), 9(d))
Super-Gaussian (3-d order)	$7 \leqslant N \leqslant 15$, unchirped or chirped in the wide range corresponding to particular value of N.	–
	E. g. $N = 10$, $-12 \leqslant C \leqslant 4$. Examples can be found in Fig. 5, 8	

cosecond Gaussian pulses are used (e.g. ~ 5 ps) the necessary conditions $N > 3$ in TSP-regime and $N \geqslant 7$ in SSP-regime for triangular pulse formation lead to the following minimal pulse energies required in the TrueWave fiber at $\lambda = 1550$ nm: $E_0^{TSP} \geqslant 8$ pJ, $E_0^{SSP} \geqslant 45$ pJ, respectively ($\gamma_{1550} = 2.5$ (W·km)$^{-1}$). Whereas at $\lambda = 1064$ nm, due to the larger normal dispersion in single mode fibers (e.g. in Thorlabs 780HP) minimal pulse energies have to be larger to meet those conditions: $E_0^{TSP} \geqslant 36$ pJ, $E_0^{SSP} \geqslant 0.2$ nJ, respectively ($\gamma_{1064} = 3.6$ (W·km)$^{-1}$). However, modern commercially available picosecond fiber lasers are able to reach these pulse energies easily.

Application of femtosecond pulses for nonlinear reshaping looks much more attractive. If femtosecond Gaussian pulses are used (e.g. 200 fs) then the dispersion length in TrueWave fiber at $\lambda = 1550$ nm is $L_D = 3.6$ m. Thus, the required fiber length for pulse reshaping is sufficiently smaller in this case: a few meters for triangular pulse formation in the steady-state propagation regime and even less than 1 meter for transient-state propagation regime. At 800 nm in single mode fibers such as Thorlabs 780HP the dispersion length is even smaller $L_D = 37$ cm due to the larger normal dispersion ($\beta_2 = 39$ ps^2/km). Therefore, pulse reshaping at 800 nm with femtosecond pulses requires applications of very short single mode fibers: a few tens of centimeters in the transient-state propagation regime and about one meter in the steady-state propagation regime. In this case one can realize really compact scheme of pulse reshaping based on application of normal dispersive optical fibers. If femtosecond Gaussian pulses are used (200 fs) then the necessary conditions $N > 3$ TSP-regime and $N > 7$ SSP-regime for triangular pulse formation lead to the following minimal pulse energies required in the TrueWave fiber @1550 nm: $E_0^{TSP} \geqslant 0.2$ nJ, $E_0^{SSP} \geqslant 1.1$ nJ, respectively. Whereas at 800 nm minimal pulse energies have to be larger to meet those conditions: $E_0^{TSP} \geqslant 0.4$ nJ and $E_0^{SSP} \geqslant 2.3$ nJ, respectively, for the fiber Thorlabs 780HP ($\gamma_{800} = 12$ (W·km)$^{-1}$). Modern commercially available femtosecond Ti:Sapphire and fiber lasers are able to reach these pulse energies.

Finally we present an estimation of triangular pulse formation in real fiber such as conventional single mode fiber Thorlabs 780HP, intended for application at near infrared wavelengths. It is considered triangular pulse formation in the steady-state regime from initial unchirped

#224299 - $15.00 USD Received 2 Oct 2014; revised 1 Nov 2014; accepted 1 Nov 2014; published 14 Nov 2014

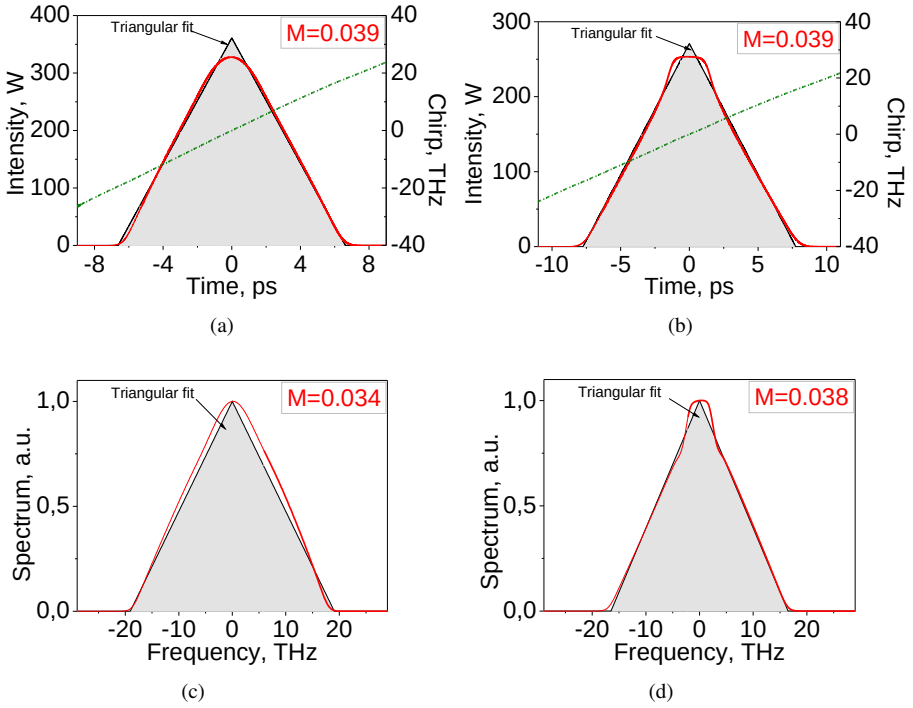

Fig. 9. Triangular pulses produced in the Thorlabs 780HP fiber. The left column shows results ((a) - temporal intensity and chirp (green curve), (c) - spectrum) for triangular pulse generated in the steady-state regime at the fiber length 1.4527 m ($\xi = 4$) from initial unchirped Gaussian pulse ($N = 7$, $E_0 = 2.39$ nJ, FWHM=200 fs). Right column ((b), (d)) shows triangular pulse generated in the steady-state regime at the fiber length 1.9435 m ($\xi = 6$) from initial unchirped secant pulse ($N = 6$, $E_0 = 2.101$ nJ, FWHM=200 fs). The insets located in the upper right corner show the amount of misfit parameter M. Red curves show corresponding triangular fits.

Gaussian and the hyperbolic secant pulses with central wavelength $\lambda_0 = 800$ nm. The parameters of the pump pulses are chosen to be similar to those one produced by typical Ti:Sapphire lasers or Er^{3+}-doped fiber lasers with second harmonic generation. Particularly pulse duration is 200 fs and pulse energy equal to a few nanojoules.

The fiber parameters at 800 nm used in NLSE, Eq. (1), are: $\beta_2 = 39.73$ ps^2/km, $\beta_3 = 2.62 \times 10^{-2}$ ps^3/km, $\gamma = 12$ (W·km)$^{-1}$, and $\alpha = 8.0589 \times 10^{-4}$ m^{-1} . Dispersion coefficients β_n are calculated from $D(\lambda)$, [ps/(nm·km)], whereas nonlinear coefficient γ is calculated from the mode field diameter of the fiber using nonlinear refractive index of the silica $n_{SiO_2} = 3 \times 10^{-20}$ m^2/W.

Fig. 9 shows characteristics of triangular pulses obtained in the steady-state regime from initial unchirped secant and Gaussian pulses. Fig. 9 clearly shows that applying initial Gaussian or secant pulses we can obtain indeed pulses close to the ideal triangular profile both in spectral and temporal domains. One can see that the main deviations form ideal triangular waveform appear preliminary in the top of the pulse profile. In all cases the top is not perfectly sharp as compared to the ideal triangular profile. However, the most part of pulse edges is nearly linear. One has to note also that the chirp of obtained triangular pulses is also perfectly linear here.

Results shown in Fig. 9 are obtained neglecting the fourth order dispersion (FOD) and in-

#224299 - $15.00 USD Received 2 Oct 2014; revised 1 Nov 2014; accepted 1 Nov 2014; published 14 Nov 2014

Table 2. Comparisons of contributions of the fourth order dispersion and Raman intrapulse scattering into distortion of triangular pulses in the Thorlabs 780HP fiber

Incident Pulse Shape	Original misfit parameter		Misfit including FOD		Misfit including FOD and Raman scattering	
	M_τ	M_ω	M_τ	M_ω	M_τ	M_ω
Gaussian	0.039	0.034	0.039	0.033	0.043	0.032
Secant hyperbolic	0.039	0.038	0.033	0.033	0.032	0.032

trapulse Raman scattering. The role of the FOD in transformation of parabolic optical pulses to triangular wave forms in the normal dispersion regime has been addressed in [26]. It has been shown that FOD may be one ingredient leading to the emergence of triangular pulse in a nonlinear system. However, it should be observed that analysis made in [26] embraces only transient-state propagation regime (particularly $\xi \ll 1$), and thus conclusions made are valid strictly for these conditions. Nevertheless one can expect that accounting for the FOD could be important in cases considered here as well. Given also the spectral extend of the resulting pulses that are shown in Fig.9 one can expect an influence of intrapulse Raman scattering. Thus, both factors can potentially destroy conditions for triangular pulse formation. In order to clarify the contribution of these phenomena in our case we made simulation of triangular pulse formation for the case shown in Fig.9, taking into account FOD only, and both factors as well, the FOD and the Raman intrapulse scattering. We found no noticeable contributions. The shapes of the spectra and wave forms do not changed; the only minor variations appear, which are not observable in the linear scale but led to minor change (tenth part of percent) of the misfit parameters; they are shown in Table 2. It can be noted a tendency to decreasing of misfit parameter when including higher-order nonlinear and dispersion effects into account. Thus simulations without FOD and Raman intrapulse scattering allow us talk about an utmost estimation of the conditions for triangular pulse formation; knowing these estimation we can be sure that pulses will be obtained in real fibers.

7. Conclusion

We have investigated numerically formation of ultrashort triangular pulses by means of passive nonlinear reshaping in normal dispersive optical fibers. The conditions for triangular pulses formation both in the transient-state regime and in the steady-state regime were found depending on the initial pulse shape, chirp and soliton order. It was shown that in the transient-state regime triangular pulses can be obtained only from Gaussian pulses when $N > 3$ with negative chirp (e.g. $-8 \leqslant C \leqslant -2$, $N = 10$) and from unchirped or chirped super-Gaussian pulses when $7 \leqslant N \leqslant 15$ (e.g. $-12 \leqslant C \leqslant 4$, $N = 10$). Whereas nor soliton order variation nor chirp variation does not provide formation of triangular pulses form secant waveform in the transient-state regime.

In the steady-state regime triangular pulses can be obtained from both unchirped Gaussian ($N \geqslant 7$) and secant ($N \geqslant 3$) initial pulses for sufficiently large value of soliton order. In general application of secant pulses is more preferable for obtaining of triangular pulses. For secant initial pulses smaller soliton order is required for triangular pulse formation and misfit parameter is slightly lower. In the steady-state regime in general the adding of initial chirp increases the deviation form triangular waveform as compared to unchirped initial pulses. However, there is the range of initial chirp $-0.5 \leqslant C \leqslant 0.4$ ($N = 10$) for initial Gaussian pulse and $-0.8 \leqslant C \leqslant 0.5$ ($N = 10$) for initial secant pulse where pulse in the stead-state regime preserves triangular pro-

#224299 - $15.00 USD Received 2 Oct 2014; revised 1 Nov 2014; accepted 1 Nov 2014; published 14 Nov 2014

file both in temporal and spectral domain. Whereas nor soliton order variation nor chirp variation does not provide formation of triangular pulses from super-Gaussian (3-rd order) pulses in the steady-state regime.

Finally, we have shown the possibility of generating triangular pulses in the steady-state regime from unchirped femtosecond Gaussian and hyperbolic secant pulses applying 1-2 m of the conventional single mode fiber Thorlabs 780HP. Both pulse temporal shape and spectrum are close to the triangular waveform and remain triangular shape during subsequent pulse propagation in the fiber, whereas pulse chirp is linear.

Acknowledgments

This work is supported by University of Guanajuato (projects DAIP-334/13 and DAIP-192/13), by Secretaría de Educación Pública via program PROMEP (project UGTO-PTC-371).

#224299 - $15.00 USD Received 2 Oct 2014; revised 1 Nov 2014; accepted 1 Nov 2014; published 14 Nov 2014